Cinpar 2016

PROGRAMME

XII INTERNATIONAL CONFERENCE ON
STRUCTURAL REPAIR AND REHABILITATION
PORTO | PORTUGAL
26-29 OCTOBER 2016

U.PORTO FEUP FACULDADE DE ENGENHARIA UNIVERSIDADE DO PORTO
CONSTRUCT
LESE Laboratório de Engenharia Sísmica e Estrutural
instituto da construção
UNIVERSIDADE ESTADUAL VALE DO ACARAÚ

Conference scope

Structural engineering experts in strengthening and repair of structures need to have a comprehensive knowledge over a set of issues: the materials used (masonry, adobe, timber, steel, concrete and others); the geometrical properties of the structures; the available surveying techniques for determining the physical and mechanical properties of the materials; the behaviour of the structural elements and the types of validated strengthening and repair techniques available for the different types of constructions.

Over the last years, the advances in structural expertise have revealed a substantial appeal from the intervenients and their roles in the construction industry as well as the appearance of new materials and construction techniques. Recent construction market forecasts indicate a considerable growth in the investment on the strengthening and repair activity (EuroConstruct Statistics).

The CINPAR 2016 international conference is an opportunity for the participants to acquire knowledge on new materials, techniques and construction technologies, and to exchange personal experiences on strengthening and repair of structures.

Principal aims

Present and discuss the surveying and diagnosis techniques for material characterization;

Present and discuss common construction defects;

Identify and analyse the main causes of defects, whose knowledge is crucial for a successful repair action;

Present materials used in the repair and strengthen existing structures;

Present and discuss techniques to repair and strengthen existing structures;

Promote the communication and sharing of knowledge among different professionals working on this field;

To identify, discuss and encourage future research directions for the strengthening and repair of structures.

For the Organizing Committee, it is a pleasure to welcome keynote-speakers, authors and other participants to the XII International Conference on Structural Repair and Rehabilitation and to the city of Porto. We hope that you will profit from the scientific program, from the interaction with colleagues and that you will enjoy the charming city of Porto.

COMMITTEES

Executive Committee

Humberto Varum – FEUP (Portugal)
António Arêde – FEUP (Portugal)
Esequiel Mesquita – FEUP (Portugal)
Esmeralda Paupério – IC (Portugal)
Hugo Rodrigues – IPL (Portugal)
José Melo – FEUP (Portugal)
Xavier Romão – FEUP (Portugal)

Advisory Committee

Francisco Carvalho – UVA (Brazil) - *Coordinator*
Alexandre Bertini – UFC (Brazil)
Angel Oshiro – UTN (Argentina)
Bernardo Fonseca Tutikian – UNISINOS (Brazil)
César Daher – IDD (Brazil)
César de Luca – IDD (Brazil)
Eduardo Ballán Ballán – UCJC (Spain)
Gibson Rocha Meira – IFPB (Brasil)
Humberto Varum – FEUP (Portugal)
Jorge Sota – LEMIT (Argentina)
Luis Traversa – LEMIT (Argentina)
Maria Positieri – UTN (Argentina)
Pablo Maturana Barahona – PUC (Chile)
Petr Stepánek – VUTBR (Czech Republic)
Soledad Gomez Lorenzini – PUC (Chile)

Local Organizer Committee

Humberto Varum – FEUP (Portugal)
Alexandre Costa – ISEP (Portugal)
Aníbal Costa – UA (Portugal)
António Arêde – FEUP (Portugal)
Bruno Quelhas – FEUP (Portugal)
Celeste Almeida – FEUP (Portugal)
Esequiel Mesquita – FEUP (Portugal)
Esmeralda Paupério – IC (Portugal)
Hipólito Sousa – FEUP (Portugal)
Hugo Rodrigues – IPL (Portugal)
João Guedes – FEUP (Portugal)
José Melo – FEUP (Portugal)
Mário Marques – FEUP (Portugal)
Miguel Castro – FEUP (Portugal)
Nelson Vila Pouca – FEUP (Portugal)
Patrício Rocha – IPVC (Portugal)
Pedro Delgado – IPVC (Portugal)
Vasco Freitas – FEUP (Portugal)
Xavier Romão – FEUP (Portugal)

Secretariat

Maria Amélia
Maria de Lurdes Lopes
Manuel Carvalho

Organization

Scientific Committee

Abílio de Jesus (INEGI-FEUP), Portugal
Alessandra Aprile (UFerrara), Italy
Alessandra Marini (UBergamo), Italy
Alexandre Bertini (UFC), Brazil
Alexandre Costa (ISEP), Portugal
Alicia Fortis (UCJC), Spain
Almir Sales (UFSCar), Brazil
Alper Ilki (ITU), Turkey
Ana Velosa (UA), Portugal
Anabela Paiva (UTAD), Portugal
André Barbosa (OSU), USA
Angel Oshiro (UTN-FRC), Argentina
Aníbal Costa (UA), Portugal
António Arêde (FEUP), Portugal
Antonio Borri (UPeruggia), Italy
Antonio Formisano (UNaples), Italy
Artur Pinto (ELSA-JRC), Italy
Arturo Tena (UAM), Mexico
Bernardo Tutikian (UNISINOS), Brazil
Bruno Briseghella (Fuzhou Univ), China
Camillo Nuti (URoma3), Italy
Carlos Baronetto (UNC- UTN), Argentina
Carlos Chastre (UNL), Portugal
Carlos Félix (ISEP), Portugal
Carlos Marín (UC), Chile
Carmen Andrade (CISDEC/DUREM), Spain
César Daher (IDD), Brazil
César de Luca (IDD), Brazil
Daniel Oliveira (UM), Portugal
Débora Ferreira (IPB), Portugal
Delgado Rodrigues (LNEC), Portugal
Edinson Guanchez (UCarabobo), Venezuela
Eduardo Ballán (UCJC), Spain
Eduardo Cabral (UFC), Brazil
Eduardo Júlio (IST), Portugal
Enio Pazini (UFG), Brazil
Enrico Spacone (UChieti-Pescara), Italy
Ezio Giuriani (Univ. Brescia), Italy
Fernanda Rodrigues (UA), Portugal
Fernando Pinho (UNL), Portugal
Francisco Carvalho (UVA/IEMAC), Brazil
Fulvio Parisi (UNaples), Italy
Gibson Meira (IFPB), Brazil
Giorgio Monti (URome), Italy
Giovanni Fabbrocino (UMolise), Italy
Graciela Maldonado (UTN), Argentina
Guido Camata (UChieti-Pescara), Italy
Guillermo Martínez (UMSNH), Mexico
Gustavo Ayala (UNAM), Mexico
Hipólito de Sousa (FEUP), Portugal
Hugo Rodrigues (IPL), Portugal
Humberto Varum (FEUP), Portugal
Ignacio Lombillo (UCantabria), Spain
Jaime Gálvez (UPM), Espanha
Jitendra Agarwal (UBristol), UK
João Appleton (A2P), Portugal
João Lanzinha (UBI), Portugal
João Mascarenhas Mateus (FAUL), Portugal
João Miranda Guedes (FEUP), Portugal
Jorge Branco (UM), Portugal
Jorge de Brito (IST), Portugal
Jorge Sota (LEMIT), Argentina
José Aguiar (FAUTL), Portugal
José Amorim Faria (FEUP), Portugal

Scientific Committee

José Correia (INEGI), Portugal
José Jara (UMSNH), Mexico
Juan García (Univ Jaume I), Spain
Kleber Franke Portella (Inst. Lactec), Brazil
Lorenzo Jurina (P Milan), Italy
Luigi Ascione (USalerno), Italy
Luís Romera (UCoruña), Spain
Luis Villegas (UCantabria), Spain
Luiz Branco (FUMEC), Brazil
Manuel Fernández (UPM), Espanha
Marcial Blondet (PUC), Peru
María Inés Sastre (UNSA), Argentina
Maria Positieri (UTN-FRC), Argentina
Maurizio Piazza (UTrento), Italy
Mehrtash Motamedi (Islamic Azad Univ), Iran
Michelangelo Laterza (UBasilicata), Italy
Miguel E. Ruiz (UNCórdoba), Argentina
Miguel Pando (UNCCharlotte), USA
Nelson Vila Pouca (FEUP), Portugal
Néstor Ortega (UNS), Argentina
Nicola Tarque (PUC), Peru
Pablo Maturana (PUC), Chile
Panagiotis Asteris (SPTE), Greece
Paolo Riva (UBergamo), Italy
Paulo Cruz (UM), Portugal
Paulo Fernandes (IPL), Portugal
Paulo Helene (USP), Brazil
Paulo Lourenço (UM), Portugal
Petr Stepánek (VUTBR), Czech Republic
Radu Vacareanu (UTCB), Romania
Rafael Aguilar (PUC), Peru
Raimundo Mendes da Silva (FCTUC), Portugal
Raúl Zerbino (LEMIT- UNLP), Argentina
Robson Gaiofatto (UCPetrópolis), Brazil
Romeu Vicente (UA), Portugal
Rosário Veiga (LNEC), Portugal
Rui Póvoas (FAUP), Portugal
Sergio Lagomarsino (UGenoa), Italy
Soledad Gomez (PUC), Chile
Thanasis Triantafillou (UPatras), Greece
Tiago Pinto (UTAD), Portugal
Tiziana Rossetto (UCL), UK
Válter Lúcio (UNL), Portugal
Vasco Freitas (FEUP), Portugal

[EN] Strengthening slabs for punching shear using fiber reinforced polymer
Carlos Moreno, Débora Ferreira, Sarmento Ana

[EN] Analysis of reinforcement techniques for partition walls subjected to vertical deformations of concrete slabs
Hipólito Sousa, Rui Sousa

[EN] Life cycle cost optimization of a shotcrete tunnel lining
Petr Štěpánek, Ivana Lanikova, Jakub Venclovsky

[EN] Bond-slip monitoring of RC through optical fibre sensor
Esequiel Mesquita, Paulo Antunes, Nélia Alberto, José Melo, Carlos Marques, Paulo André, Humberto Varum

09:30-11:00 **SESSION S27-A-3 (Room 3)**

Chairs: María Soledad Gómez, João P. Miranda Guedes

[PT] Restauração da Catedral de Petrópolis
Ana Kyzzy Fachetti, Érika Machado, Robson Gaiofatto

[CA] El deterioro de las fábricas de piedra de la Catedral de León: La utilización de azufre en el retacado de grapas y tochos en las intervenciones del siglo XIX
Jorge Diez Garcia-Olalla

[CA] Metodología de rehabilitación de patrimonio histórico en la ciudad de Skikda, Argelia
Montserrat Bosch González, Joan Ramon Rosell Amigó, Oriol Marín Gordi, Albert Albareda-Valls, Jordi Maristany Carreras

[CA] Recuperación, restauración y protección del patrimonio del Cementerio Viejo de Concordia
Maria Alejandra Bruno, Vilma Gabriela Rosato, Fabricio Altamirano, Emanuel Lizalde, Jorge Daniel Sota

[CA] Puesta en valor del palacio Arruabarrena, Concordia, Entre Ríos, Argentina
Jorge Daniel Sota, María Alejandra Bruno, Luis P. Traversa, Fabricio Altamirano, Emanuel Lizalde

11:00-11:30 Coffee-Break

XII Congresso Internacional sobre Patologia e Reabilitação de Estruturas
XII International Conference on Structural Repair and Rehabilitation
26-29 October, 2016, Porto, Portugal

Strengthening slabs for punching shear using fibre reinforced polymer

Carlos MORENO[1], **Débora FERREIRA**[2], Ana SARMENTO[3]

[1] University of Applied Sciences and Arts Western Switzerland, Geneva, Switzerland, carlos.moreno@hesge.ch
[2] Polytechnic Institute of Bragança, Bragança, Portugal, debora@ipb.pt
[3] University of Porto, Porto, Portugal, ams@fe.up.pt

Abstract: Punching is generally associated to the application of concentrated loads or to the presence of columns. One of the main concerns related to flat slabs is its punching shear capacity at slab-column connection, which is subjected to a very complex three-dimensional stress state. Provided that bending capacity is installed, punching shear failure is characterized by the development of a truncated cone shaped surface at the slab-column connection.

Recurrently, there is the need to strengthen existing flat slabs against punching shear failure. The use of fibre-reinforced polymer (FRP) is an innovative technology to strengthen concrete structures. In this paper, punching shear strengthening of flat slabs using carbon fibre reinforced polymer (CFRP) is studied.

The experimental programme carried out by the authors includes four normal strength concrete slabs (1100×1100×100 mm^3), with and without shear reinforcement, submitted to punching under a concentrated load. One of the specimens included typical bent-down bars as shear reinforcement. Among available strengthening practices, the technique that consists on gluing CFRP on concrete surface have been tested within current experimental programme. Moreover, the near surface mounted (NSM) technique has also been tested within current experiments. Finally, a fourth specimen served as reference. The effects of shear reinforcement and of CFRP enhancing punching shear capacity are observed.

Keywords: Punching shear, CFRP, NSM, Experimental test

1. Introduction

Punching shear can result from a concentrated load or reaction acting on a relatively small area, called the loaded area, of a slab or a foundation. This type of failure is usually both brittle and catastrophic since it may generate the global collapse of the structure due to the increasing load transferred to neighbouring columns and to the slabs located underneath. The load carrying capacity of reinforced concrete (RC) slabs may be compromised for a number of reasons, including structural damage, design errors, building code changes and alteration of functional use.

Two strengthening techniques enhancing directly the bending capacity of slab-column connections are employed. The collateral increase in the ultimate punching shear capacity is analysed. The use of carbon fibre reinforced polymers (CFRP) on structural repair and strengthening has continuously increased during the last years due to the following main advantages of this composite material when compared to conventional materials like steel and concrete: low specific weight, easy installation, high durability and tensile strength, electromagnetic permeability, and practically unlimited availability regarding size, geometry and dimensions ACI (2008).

The most widely used technique aiming to increase load carrying capacity is to apply CFRP plates on the tension surface of the RC slab as externally bonded (EB) reinforcement. CFRP laminates and sheets are generally applied on the faces of the elements to be strengthened configuring which is commonly designated as the EB reinforcing technique. The research carried out up to now has revealed that this method cannot mobilize the full tensile strength of CFRP materials due to the occurrence of premature debonding phenomenon, Nigro, Ludovico & Bilotta (2008). Due to the fact that CFRP is often directly exposed to the weathering conditions, the reinforcing performance of this technique should be accounted

for. EB systems are as well vulnerable regarding fire action and vandalism acts. Alternatively, the near surface mounted (NSM) technique, which consists of cut-in openings strengthened with CFRP materials, can be used. This technique was used in some practical applications, Barros *et al.* (2006), and several benefits were pointed out. In order to assess the efficacy of this strengthening system as regards structural elements failing in punching shear, flat slab specimens were tested. The carried out tests are described and the most significant outcomes are presented and analysed. Experimental results are also compared with design code predictions regarding the punching shear strength.

2. Experimental programme

2.1 Test specimens

Current experimental programme includes 4 RC square flat slab specimens 1100×1100 mm^2 wide and 100 mm height, which were designed so as the bending capacity prevail over the punching shear strength in order for slabs to fail in shear. The ordinary reinforcement ratio remained unchanged for all the tested slabs. Full details of specimen's geometry are presented in Figure 1 where the ordinary reinforcement has been omitted in both the CFRP strengthened slabs for interpretation convenience.

The first specimen, denoted BC01, served as the non-strengthened reference slab. The second specimen, BCA1, included typical steel bent-down bars as punching shear reinforcement. The CFRP strengthening techniques were used in the third specimen, BCN1, which include 16 NSM cut-in in each direction, and in the EB specimen, denoted BCG1, on which 6 CFRP laminates were bonded in each direction. Both the CFRP strengthened specimens were designed so as approximately similar effective reinforcement ratios (ρ_{tot}) were installed, see Table 1 (refer to Figure 1 for axis orientation), Table 2, and Moreno *et al.* (2015).

Table 1 – Main reinforcement ratio and geometry for BCN1 specimen

Layer	Material	Direction	d (mm)	ρ_l (%)	d (mm)	ρ_{st} (%)	d_{st} (mm)	d_{eq} (mm)	ρ_{tot} (%)
1	Steel	x	68	1.33	72.0	-	-	76.7	2.07
2		y	76						
3	CFRP	y	85	-	-	0.45	90.0		
4		x	95						

Table 2 – Main reinforcement ratio and geometry for BCG1 specimen

Layer	Material	Direction	d (mm)	ρ_l (%)	d (mm)	ρ_{st} (%)	d_{st} (mm)	d_{eq} (mm)	ρ_{tot} (%)
1	Steel	x	68	1.33	72.0	-	-	78.4	2.08
2		y	76						
3	CFRP	y	100.6	-	-	0.32	101.2		
4		x	101.8						

In Table 1 and Table 2, d is the mean effective depth of the slab, ρ_l is the ordinary reinforcement ratio, ρ_{st} is the strengthening reinforcement ratio, d_{st} is the distance between the compressed face and the centroid of the CFRP strengthening elements, d_{eq} is the equivalent effective depth and ρ_{tot} is the effective reinforcement ratio.

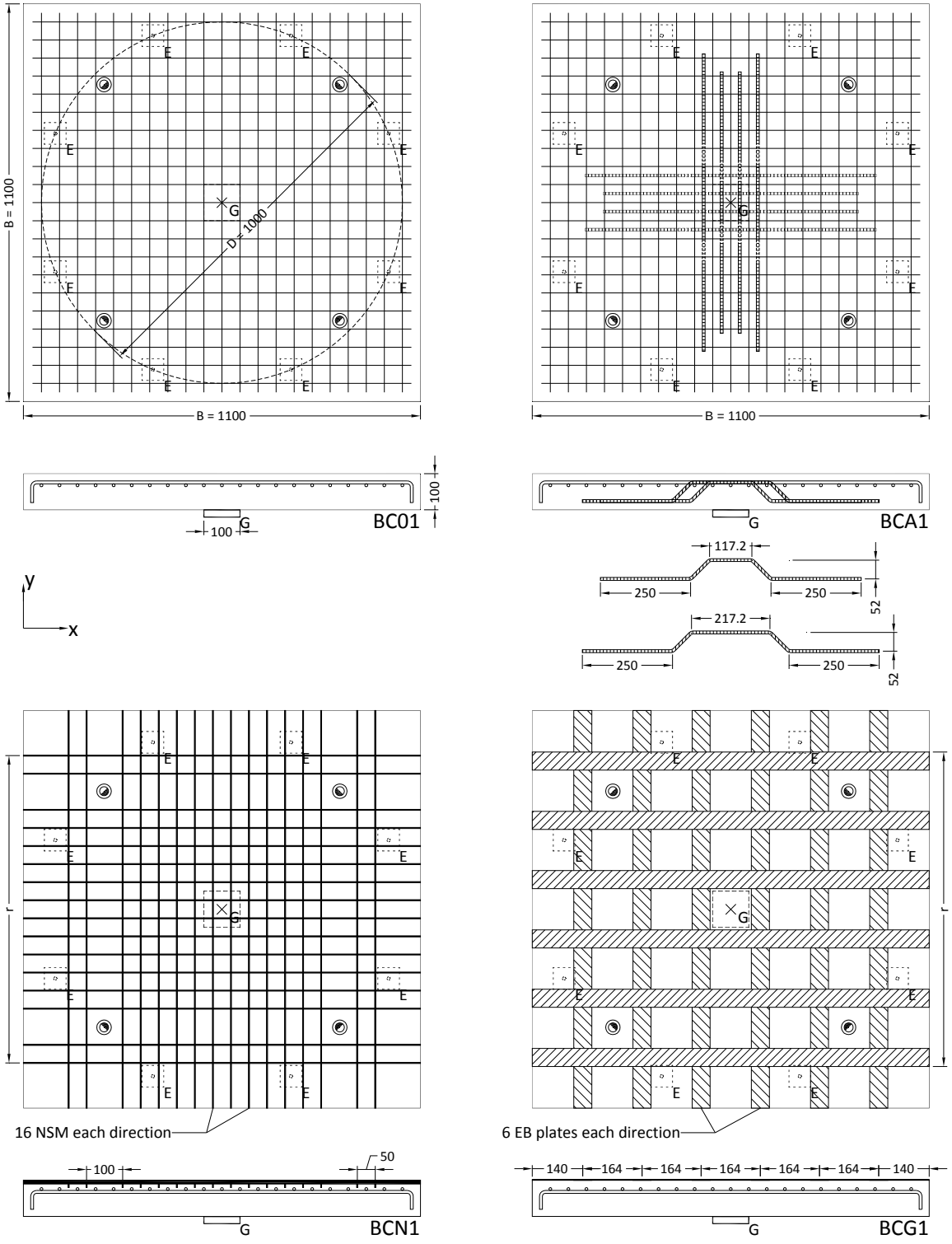

Figure 1 – Geometry of tested slabs (dimensions in mm)

All the current specimens were reinforced on the top (tensile) side with orthogonal bending reinforcement using 8 mm diameter rebar spaced 50 mm. The main bars were folded up at both ends in order to promote better anchorage. The ratio ρ_l of ordinary reinforcement was 1.33% for all the tested specimens. A 20 mm concrete cover was guaranteed by using plastic rebar-to-formwork spacers.

Regarding BCA1 specimen, shear reinforcement comprising four bent-down bars in each direction were used spaced 50 mm. Shear reinforcement bars (8 mm diameter bars similar to the main reinforcement) were well anchored at their extremities and placed in two perimeters perpendicularly to the column face as shown in Figure 1. The first perimeter of shear elements was positioned at a distance of approximately half effective depth (d/2) from the column face. The radial spacing of shear reinforcement perimeters was taken as $s_r \approx 0.7d$. According to Hallgren (1996) the ratio of ordinary reinforcement should be modified (increased) with the part of the steel bent-down bars which act as main bending reinforcement over the loaded area (100×100×20 mm^3 steel plate denoted G in Figure 1).

2.2 Material properties

The tensile mechanical properties of the steel reinforcement were derived from representative samples testing. The yield and ultimate strength as well as the Young's modulus were measured and are as given in Table 3.

Table 3 – Material properties of bending and shear reinforcement steel

Diameter (mm)	Yield strength, f_{ym} (N/mm^2)	Ultimate strength, f_{um} (N/mm^2)	Young modulus, E_s (kN/mm^2)
8	535	650	200

The concrete was designed to have a 28-day cube compressive strength of 30 MPa using 19 mm maximum aggregate size and a 0.55 free water-cement ratio. A 1% cement content of Sika ViscoCrete super-plasticiser was included in the concrete mix. A CEM II/B-M (T-LL) 42.5 cement was employed. Table 4 presents the average mechanical properties obtained on concrete samples which were tested on the experiment day of the respective slab specimen.

Table 4 – Mechanical properties of concrete mix

Slab	γ_{cm} (kN/m^3)	f_{cm} (N/mm^2)
BC01	23.3	42.6
BCA1	23.4	35.3
BCN1	24.0	26.4
BCG1	23.0	27.0

The used CFRP plates were S&P CFK 150/2000 manufactured in Portugal by S&P Clever Reinforcement. These carbon laminates were used together with adhesive S&P Resin Epoxy 55 certified in accordance with CEN-EN 1504-4 (2004). Material properties of the CFRP plates used in current experimental tests are given in Table 5 and S&P (2014).

Table 5 – Material properties and geometry of CFRP laminates

Parameter	BCN1 specimen	BCG1 specimen
Cross section (mm^2)	2.8×10	50×1.2
Modulus of elasticity, E_{st} (kN/mm^2)	165	165
Theoretical tensile strength at 0.8% elongation (N/mm^2)	1300	-
Recommended tensile strength for the design (N/mm^2)	-	1650
Tensile strength (N/mm^2)	2000	2000

2.3 CFRP strengthened specimens' preparation

The CFRP strengthened slabs were prepared following the instructions of the manufacturer. Regarding BCN1 slab, the slots of 5.5×20 mm^2 and 5.5×10 mm^2 were obtained using a circular saw, as shown in Figure 2. For BCG1 specimen, a surface grinder was passed back and forth along pre-aligned paths until a uniform exposure of aggregate was achieved, see Figure 3. A vacuum cleaner allowed a clean surface from dust and loose particles to be obtained.

Figure 2 – BCN1 slots cutting

Figure 3 – BCG1 surface prior to CFRP gluing

2.4 Test procedure and instrumentation

All tests were conducted under concentrated loading (100×100 mm^2) and simply supported on eight points (60×60×10 mm^3 steel plates denoted E in Figure 1) equally spaced along a D = 1000 mm diameter perimeter (see Figure 1). Tests were performed using a servo-hydraulic test system by means of controlling the vertical force at 0.26 kN/s constant loading rate. The load was applied through a load-controlled hydraulic jack with a nominal range of 300 kN acting against a reaction strong slab.

A data acquisition system connected to a personal computer was used to control the loading and to collect test data (load, deflections and CFRP strains).

Externally, five LVDT (L1 to L5) were placed along the diameter D (see Figure 1) in order to measure the deflections of the four tested slabs. Internally, five strain gauges (A to E) were laterally glued to CFRP laminates on BCN1 slab. Three strain gauges (A to C) were glued to the top surface of CFRP laminates on BCG1 specimen. The instrumentation is located as indicated in Figure 4 where the truncated cone shaped surface taken accordingly to an estimated failure crack angle of 35 degrees is plotted.

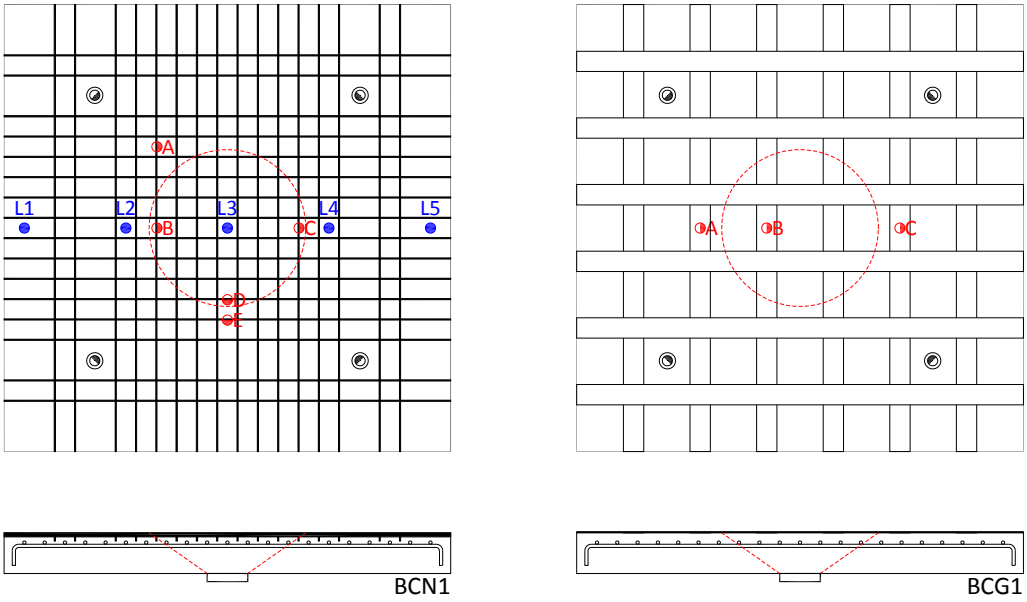

Figure 4 – Location of strain gauges and LVDT

3. Experimental results

3.1 Failure load analysis

The failure loads of the four tested slabs were predicted based on punching shear approaches of both CEB-FIP MC 90, CEB-FIP (1993), and Eurocode 2, CEN-EN 1992-1-1 (2004), considering non-strengthened specimens ($V_{Rm,ns}$ values, see Table 6) and the actual value of concrete compressive strength which was evaluated on the respective experiment day (see Table 4). Further information on predicted failure load analysis can be obtained elsewhere, Moreno *et al.* (2015, where proposals are made for both CEB-FIP MC 90 and Eurocode 2 code provisions regarding punching shear strength in order to reduce the standard deviation and the average values of the relationship between experimental and predicted punching failure loads.

All the specimens failed in punching. In the following the materials partial safety factors are taken as $\gamma_c = \gamma_s = 1$ and the concrete compressive strength is taken as the respective average value. Experimental failure loads as well as predicted failure modes are indicated in Table 6.

Table 6 – Experimental and predicted failure loads

Slab	Experimental failure load, $P_{u,exp}$ (kN)	Non-strengthened (predicted) failure load, $V_{Rm,ns}$ (kN)	Strengthened (predicted) failure load, V_{Rm} (kN)	$P_{u,exp}/V_{Rm,ns}$ (-)	$P_{u,exp}/V_{Rm}$ (-)	Predicted failure mode
BC01	176.8	173.4	-	1.02	-	Punching
BCA1	209.8	162.9	243.5	1.29	0.86	Punching
BCN1	168.7	147.8	186.8	1.14	0.90	Punching
BCG1	155.0	149.0	194.4	1.04	0.80	Punching

Design code approaches accurately predicted the failure load of the non-strengthened reference specimen BC01. Accordingly, $P_{u,exp}/V_{Rm,ns}$ ratio was computed for the remaining specimens and obtained values are indicated in Table 6. Regarding the slab reinforced with bent-down bars the enhancement on punching shear strength is estimated of about 29%. For the CFRP strengthened specimens, the NSM strengthening technique appears to be more effective (14% estimated enhancement) than EB technique (4% estimated strength increase) as regards punching capacity. Punching failure loads are consistently overestimated for shear-reinforced and CFRP strengthened specimens ($P_{u,exp}/V_{Rm}$ ratio in Table 6).

3.2 Failure pattern analysis

The failure mode of the reference specimen, BC01, which was neither shear-reinforced nor strengthened with CFRP plates, was brittle as can be seen in Figure 5 and Figure 10.

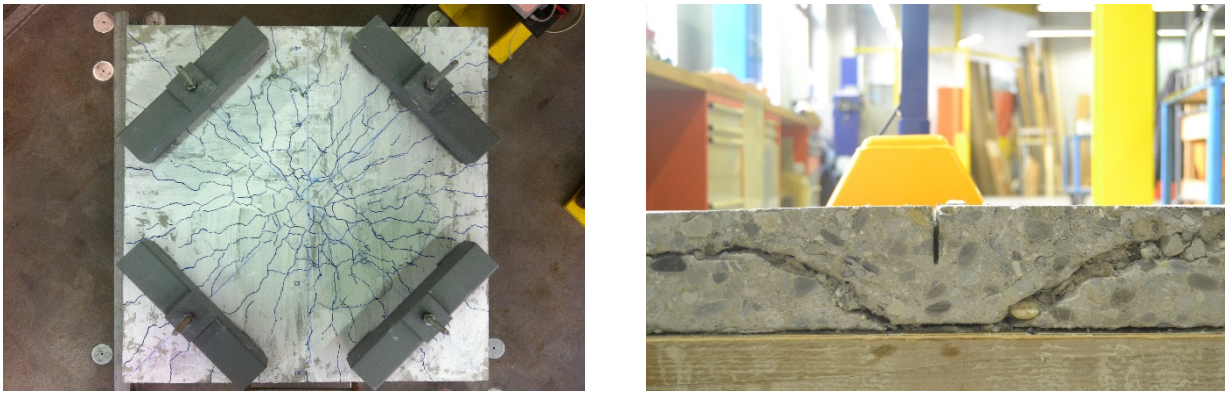

Figure 5 – Cracking pattern and internal shear crack of reference slab BC01 after failure

The failure mode of the steel shear-reinforced specimen, BA01, was also brittle as can be seen in Figure 6.

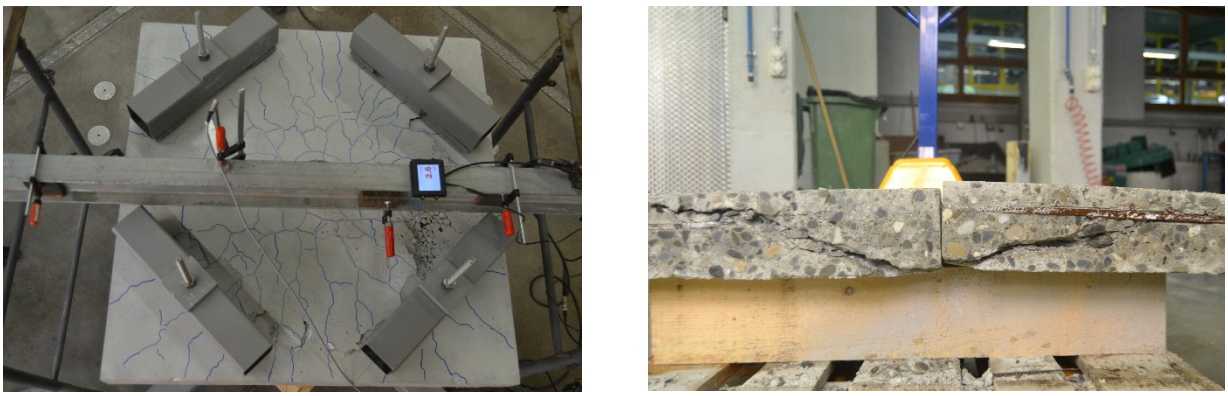

Figure 6 – Cracking pattern and internal shear crack of shear-reinforced slab BA01 after failure

Regarding both the CFRP strengthened specimens, Figure 7 and Figure 8 show the final post-experiment condition for BCN1 and BCG1 slabs, respectively. No evidence of debonding was observed in the NSM specimen. On the contrary, a pure punching shear failure was attained.

According to the literature the majority of the elements retrofitted using EB strengthening method experienced debonding as a failure method in spite of the efficiency of the strengthening technique.

As regards BCG1 specimen, no significant enhancement could hence be achieved to the overall shear stress using EB strengthening technique. A premature debonding of CFRP laminates located by the centre of the slab was identified at failure. Debonding did not actually occur at the edge of the slab but rather at an interior section. This suggests that the relative displacement perpendicular to the plane of the slab, which is due to the punching cone onset that precedes failure, set off a dowel effect that triggered the overall failure. Figure 9 confirms the above referenced occurrence.

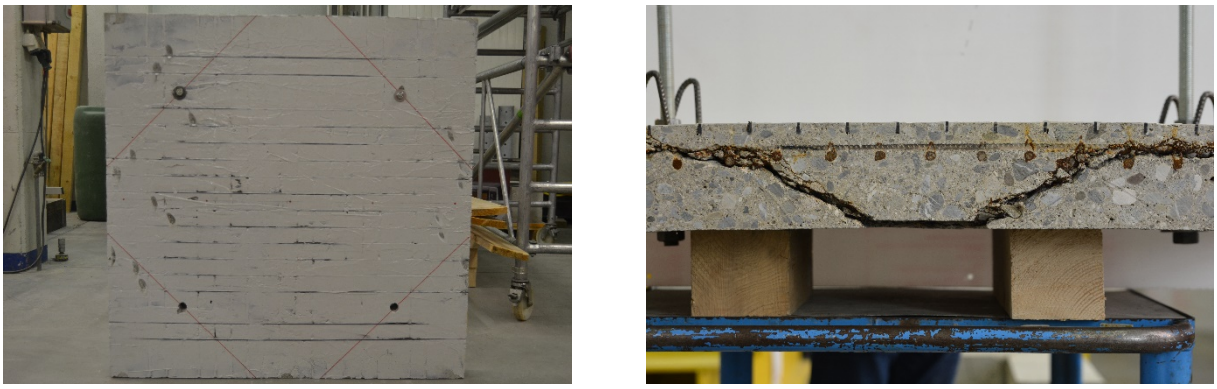

Figure 7 – Cracking pattern and internal shear crack of slab BCN1 after failure.

Figure 8 – Cracking pattern and internal shear crack of slab BCG1 after failure

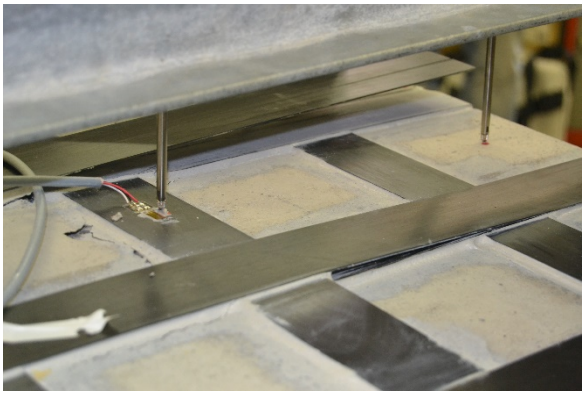

Figure 9 – Detail of local debonding on CFRP laminates of BCG1 specimen

In fact, one can point out that the anchorage length of BCG1 specimen was insufficient. However, debonding-to-tensile failure length ratios were calculated. Table 7 shows that the specific anchorage lengths related to both the CFRP strengthened specimens are quite analogous.

Table 7 – Specific anchorage lengths

Slab	CFRP strengthening technique	Debonding/tensile length (m^{-1}/m)
BCN1	NSM	0.71
BCG1	EB	0.83

3.3 Load-deflection characteristic

The deflections measured at the centre of the slabs followed an almost linear starting relationship with applied load as shown in the following (Figure 10 to Figure 13). In fact, the load-deflection relationships are nearly linear up to the first cracking occurrence in all the slabs.

No subsequent considerable reduction in stiffness was detected, except for the strengthened slabs BCN1 and BCG1 which is due to the higher effective reinforcement ratio (see section 3.1).

The load-deflection curves have thus confirmed the brittle nature of the failure of slabs collapsing in punching mode. The failure mode of the non-strengthened reference specimen BC01, which was neither shear-reinforced nor CFRP laminates strengthened, was particularly brittle as can be seen in Figure 10.

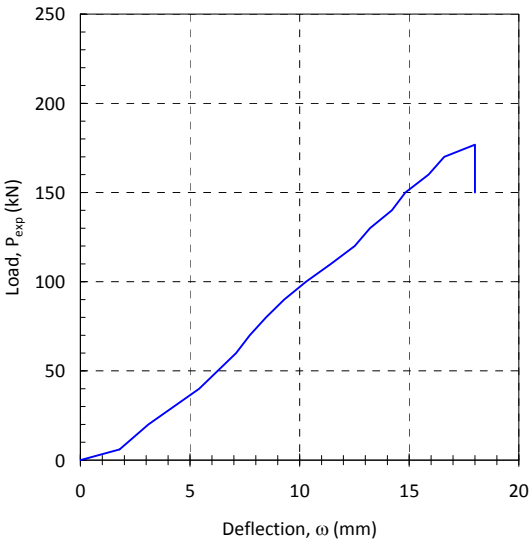

Figure 10 – Load-central deflection of the BC01 slab

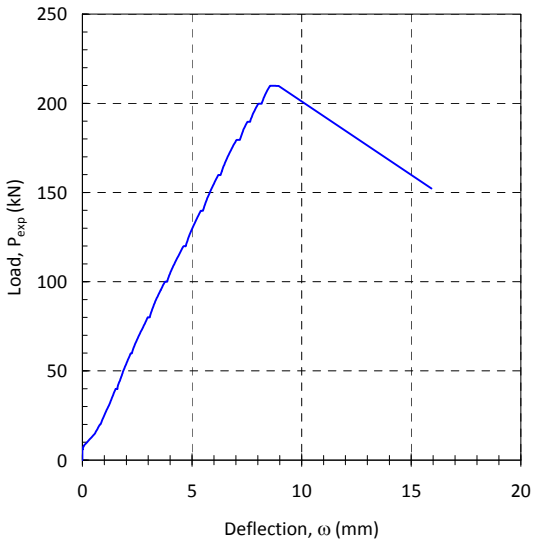

Figure 11 – Load-central deflection of the BCA1 slab

Ductility enhancement due to bent-down bars was not noticeable on the shear-reinforced slab response (Figure 11).

Concerning the NSM strengthened specimen (Figure 12), the load-deflection curve arched near the end of the experiment while the existing cracks widened and propagate towards the compression zone. The stiffness of both the CFRP strengthened specimens (Figure 12 and Figure 13) was markedly increased when compared to the non-strengthened reference specimen BC01 due to the enhanced effective reinforcement ratio. In effect, central deflections of only 3 to 4 mm were measured.

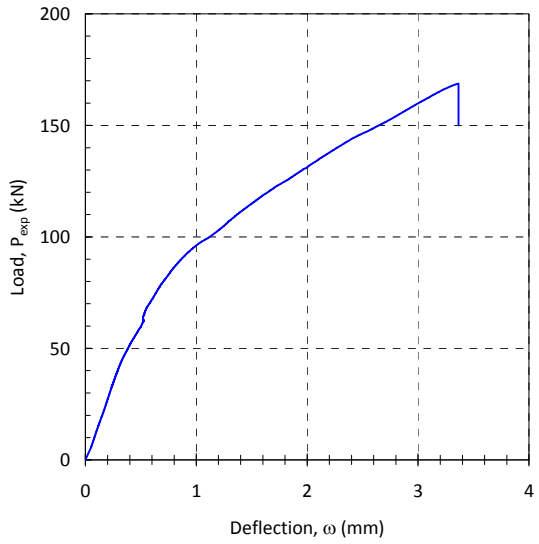

Figure 12 – Load-central deflection of the BCN1 slab

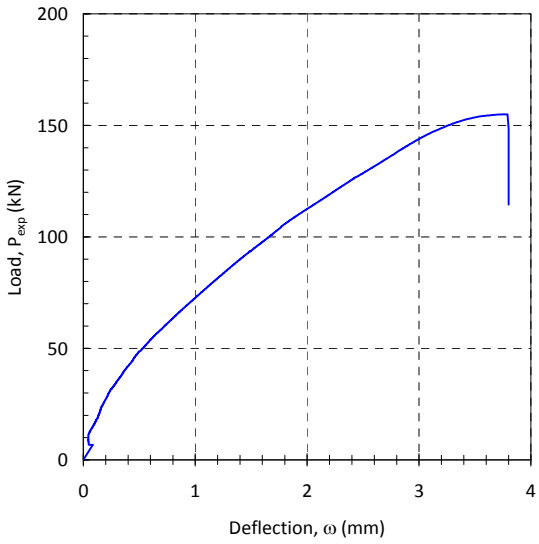

Figure 13 – Load-central deflection of the BCG1 slab

3.4 CFRP strains analysis

The load-strain relationships for the CFRP reinforcement of strengthened specimens BCN1 and BCG1 are shown in Figure 14 and Figure 15, respectively (strain gauges locations indicated in Figure 4). Assuming the strain compatibility in the strengthened slabs cross section, one can infer that ordinary reinforcement did not reach yielding on both the CFRP strengthened specimens, as maximum strains of about 0.15% to 0.20% were measured.

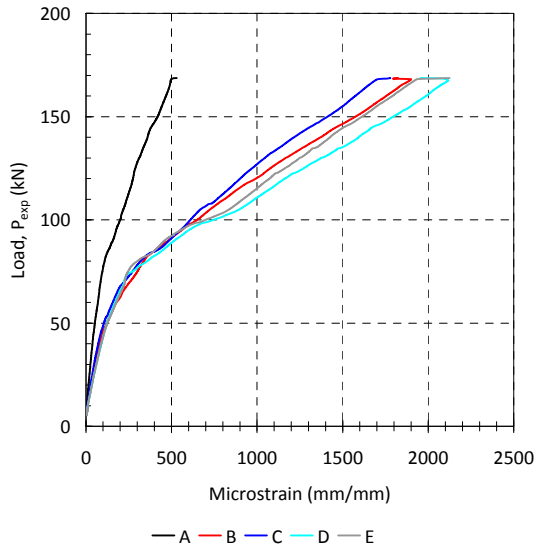

Figure 14 – Load-strain relationship for CFRP laminates of BCN1 specimen

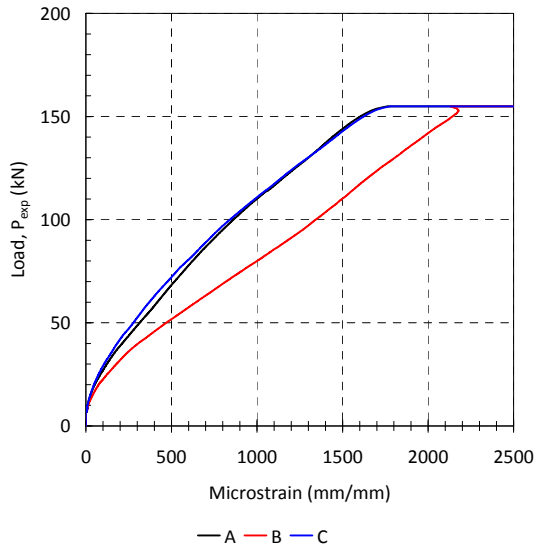

Figure 15 – Load-strain relationship for CFRP laminates of BCG1 specimen

Regarding the NSM strengthened specimen (Figure 14), CFRP strains remained of negligible magnitude until cracking initiation. Centrally located strain gauges (B to E, see Figure 4) show analogous responses. Additionally, the comparison of collected data in strain gauges A and B, which are located on the same CFRP laminate, indicate that the deformation decreases sharply with increasing distance to loaded area.

As regards the EB strengthened specimen (Figure 15), the recorded strains confirm the symmetry of the experimental test as coincident strains were obtained in strain gauges A and C.

4. Conclusions

The current work intends to assess the performance of different solutions regarding slabs' strengthening against punching. Firstly, a specimen was strengthened before casting using steel bent-down bars. For existing slabs, two different design solutions were investigated. One of them consisted in gluing CFRP laminates on slab's surface while the other design was based on introducing CFRP laminated strips into slits cute on the concrete cover, bonded to concrete using epoxy adhesive (NSM technique). In order to compare these two techniques similar CFRP reinforcement ratios were adopted.

Punching tests always show some variability. Testing of only one specimen of each slab type must therefore be handled with care. Nevertheless, further to current investigation following conclusions can be drawn:

- Good agreement is found regarding the observed-to-predicted failure load ratio $P_{u,exp}/V_{Rm}$ for the non-strengthened reference slab, BC01;
- Flat slab specimen reinforced with steel bent-down bars showed an enhanced punching shear strength of approximately 29% when compared with non-strengthened reference slab;
- The NSM specimen presented an enhanced punching shear capacity strength that can be estimated as 14%. This value should be considered relatively large when compared with results from other researchers;
- No evidence of debonding was observed in the NSM specimen. On the contrary, a pure punching shear failure was obtained;
- The NSM CFRP strips presented an enhanced performance compared to EB CFRP plates regarding punching shear failure. In the later, premature surface debonding of the laminates triggered the specimen's failure;
- On the EB CFRP specimen, no significant enhancement (4%) could be achieved to the overall shear stress using this strengthening scheme. A premature debonding of CFRP laminates was detected at the punching cone onset that preceded failure;
- Ordinary reinforcement clearly remained elastic on the four tested slabs as maximum strains of about 0.15% to 0.20% were measured on both the CFRP strengthened specimens.

Acknowledgements

The authors are appreciative to the technical staff of the LEMS – Materials and Structures Testing Laboratory – of the University of Applied Sciences Western Switzerland (HES-SO) in Geneva where current experimental programme was conducted. Authors wish as well to acknowledge the support provided by S&P Clever Reinforcement Company AG, Seewen SZ, Switzerland.

References

ACI (2008). ACI 440.2R-08 - Guide for the Design and Construction of Externally Bonded FRP Systems for Strengthening Concrete Structures, Reported by ACI Committee 440: 76.

Barros, J. A. O. d. & al. (2006). Assessing the effectiveness of embedding CFRP laminates in the near surface for structural strengthening. Construction and Building Materials 20: 478-491.

CEB-FIP (1993). Model Code 1990. Comité Euro-International du Béton. Lausanne, Thomas Telford Services Ltd: 437.

CEN (2004). EN 1992-1-1 : Eurocode 2: Design of concrete structures - Part 1-1: General rules and rules for buildings. Brussels, Central Secretariat.

CEN (2004). EN 1504-4: Products and systems for the protection and repair of concrete structures. Definitions, requirements, quality control and evaluation of conformity. Structural bonding. Brussels, Central Secretariat.

Hallgren, M. (1996). Punching Shear Capacity of Reinforced High Strength Concrete Slabs. Department of Structural Engineering. Stockholm, Sweden, Royal Institute of Technology. Doctoral Thesis: 206.

Nigro, E., Ludovico, M. D. & Bilotta, A. (2008). FRP-Concrete debonding: Experimental tests under cyclic actions. The 14th World Conference on Earthquake Engineering, Beijing, China.

Moreno, C., Ferreira, D., Bennani, A., Sarmento, A., Noverraz, M. (2015). Punching shear strengthening of slabs: CFRP and shear reinforcement. Concrete – Innovation and desig. FIB Symposium proceedings. Editors: Henrik Stang and Mikael Braestrup. Copenhagen, Denmark.

S&P (2014). Technical Data Sheet, S&P Clever Reinforcement Company AG.